ELSEVIER

Biochimica et Biophysica Acta 1383 (1998) 292–300

BIOCHIMICA ET BIOPHYSICA ACTA
BBA

Analysis of the secondary structure of the catalytic domain of mouse Ras exchange factor CDC25^{Mm}

Paola Coccetti [a], Enrico Monzani [b], Lilia Alberghina [a], Luigi Casella [b], Enzo Martegani [a,c,*]

[a] *Sezione di Biochimica Comparata, Dipartimento di Fisiologia e Biochimica Generali, Universita' di Milano, Via Celoria 26, 20133 Milano, Italy*

[b] *Dipartimento di Chimica Generale, Università di Pavia, 27100 Pavia, Italy*

[c] *III Facolta' di Scienze M.F. Naturali, Università di Milano, 21100 Varese, Italy*

Received 24 September 1997; revised 3 December 1997; accepted 9 December 1997

Abstract

The minimal active domain (GEF domain) of the mouse Ras exchange factor CDC25^{Mm} was purified to homogeneity from recombinant *Escherichia coli* culture. The 256 amino acids polypeptide shows high activity in vitro and forms a stable complex with H-*ras* p21 in absence of guanine nucleotides. Circular dichroism (CD) spectra in the far UV region indicate that this domain is highly structured with a high content of α-helix (42%). Near UV CD spectra evidenced good signal due to phenylalanine and tyrosine while a poor contribution was elicited by the three tryptophan residues contained in this domain. The tryptophan fluorescence signal was scarcely affected by denaturation of the protein or by formation of the binary complex with H-*ras* p21, suggesting that the Trp residues, which are well conserved in the GEF domain of several Ras-exchange factors, were exposed to the surface of the protein and they are not most probably directly involved in the interaction with Ras proteins. © 1998 Elsevier Science B.V.

Keywords: GDP/GTP exchange factor; Ras protein; p21*ras*-GEF interaction; Bacterial expression; Protein purification

1. Introduction

Ras proteins play an essential role in a variety of signal transduction pathways relevant for growth regulation and differentiation in eukaryotic cells [1,2].

They cycle between the active GTP-bound and inactive GDP-bound state; the intracellular levels of the Ras-GDP and Ras-GTP complexes are carefully regulated by two classes of proteins: Ras-GEF, which catalyzes GDP/GTP exchange generating the active GTP-bound form, and Ras-GAP, which stimulates the intrinsic RAS-GTPase activity promoting the hydrolysis to the inactive GDP-bound form. To date two different classes of Ras-GEFs have been identified in mammals: Sos proteins [3,4] and CDC25^{Mm}/Ras-GRF [5–7] whose Ras-activating domain is homolog to the C-terminal domain of the *Saccharomyces cerevisiae* Ras activator CDC25 protein [5]. Sos proteins (h-Sos1 and h-Sos2 in human and mSos1/mSos2 in mouse) are ubiquitously expressed in all tissues while full-length CDC25^{Mm} has

Abbreviations: MBP, maltose-binding-protein; ME, 2β-mercaptoethanol; IPTG, isopropylβD-thiogalactopyranoside; GEF, guanine nucleotide exchange factor; CD, circular dichroism

* Corresponding author. Fax: +39-2-70632811; E-mail: marteg@imiucca.csi.unimi.it

PII S0167-4838(97)00212-4

been detected at high levels only in the central nervous system where it is localized in neurons [8,9]. Ras-GRF proteins have been isolated from mouse ($CDC25^{Mm}$) [5,6], rat [7] and human [10,11]; they are quite conserved large proteins of 140 kDa containing in the N-terminal half several interesting motifs: two Plekstrin-homology (PH) domains, a Dbl-homology (DH) domain and an IQ motif [12,6,13]. Several PH domains, among which that of Ras-GRF, bind in vitro to the $\beta\gamma$ complex of trimeric G proteins [14]; in addition it has been reported that Ras activation mediated by $CDC25^{Mm}$, after addition of serum or LPA to mouse fibroblasts expressing $CDC25^{Mm}$, is pertussis toxin sensitive, suggesting that Gi proteins are involved in this signalling pathway [14–16]. Recent results identify Ras-GRF as a potential intermediary between G-protein $\beta\gamma$ subunits generated by muscarinic receptors and Ras [17]. Recently, Shou et al. [13] have been provided evidences that the IQ motif binds calmodulin and that Ras-GRF may be involved in controlling one or more neuronal process activating Ras in response to increase of intracellular calcium.

All the Ras-GEF proteins contain a conserved region of 230–240 amino acids homologous to the C-terminal domain of budding yeast CDC25 protein, called GEF domain [18,19]. This 'catalytic' domain interacts directly with the Ras proteins and is responsible for their activity of exchange factors. Expression of the C-terminal region (aa. 974–1260) of mouse $CDC25^{Mm}$ is sufficient to activate Ras proteins in vivo [5,20] while a region as short as 256 amino acids ($CDC25^{Mm}_{1005-1260}$), obtained as a fusion protein with maltose binding protein, is very active in vitro as a GDP/GTP exchanger either on mammalian H-*ras* p21 or yeast Ras2 [21].

According to a model proposed by Mistou et al. [22], the GEF domain stimulates the intrinsic low-dissociation rate of Ras-GDP through the formation of an intermediate Ras/GEF nucleotide-free complex. Actually there are few information on the mechanism of Ras/GEF complex formation and dissociation and no data regarding the structure of the GEF catalytic domain are available. Since the interaction of GEF with Ras is a key step in Ras activation (either for normal or for oncogenic Ras) the elucidation of structural and functional aspects of GEF catalytic domain is a relevant task.

As a first step to get structural information on the GDP/GTP exchange factor $CDC25^{Mm}$ we have purified the active $CDC25^{Mm}$ minimal catalytic domain (aa. 1005–1260) to near-homogeneity and its structural state was investigated using tryptophan fluorescence and circular dichroism (CD).

2. Materials and methods

2.1. Protein purifications

For the production of the minimal active domain of $CDC25^{Mm}$ (aa.1005–1260) the *Sal*I–*Xho*I fragment of plasmid pUC18/$CDC25^{Mm}$ was cloned in pMaL-cRI and expressed in *Escherichia coli* strain DH5αF′ [21].

One liter culture was grown in LB medium containing 50 μg/ml Ampicillin at 37°C. The induction was started with 0.3 mM IPTG at a cell density of 0.5 A_{600} units and continued overnight at 28°C. The cell pellet was lysed with French Press and it was resuspended in 10 ml of lysis buffer (10 mM Na_2HPO_4, 30 mM NaCl pH 7.5, 14 mM ME, 0.5 mM PMSF, 1% Triton X-100). DNAse I was added to a 100 μg/ml final concentration and the suspension was incubated at room temperature for 5 min followed by centrifugation for 20 min at 12 000 g. The resulting supernatant was mixed batchwise with 3 ml of amylose–resin (Biolabs) and gently shaken at 4°C for 50 min. After low-speed centrifugation the supernatant was discarded and the resin washed six times with buffer A (20 mM Na_2HPO_4, 150 mM NaCl pH 7.5, 0.1% TritonX-100) and with buffer B (50 mM Tris, 50 mM NaCl, 3 mM $CaCl_2$) + 0.1% Thesit (Boehringer). The MBP-$CDC25^{Mm}_{1005-1260}$ fusion protein, bound to 3 ml of the resin, was cleaved by 100 units of human thrombin (Sigma) in 5 ml of buffer B + 0.1% Thesit for 2 h at 4°C. The supernatant was recovered and the resin was washed with 3 ml of buffer B. After filtration on Minisart filter (Sartorius), the protein solution was loaded on a 1-ml MonoQ column (FPLC system, Pharmacia). The nonfused $CDC25^{Mm}_{1005-1260}$ was eluted at about 180–210 mM NaCl using a linear NaCl gradient (50–300 mM) in 50 mM Tris–HCl pH 7.5, Thesit 0.5% and 14 mM ME at a flow rate of 1 ml/min. The purest fractions

identified on SDS-PAGE were dialysed against 50 mM Tris–HCl pH 7.5, 50 mM NaCl, 14 mM ME, 50% glycerol and stored at −20°C.

H-*ras* p21 protein was produced and purified as reported in Ref. [23]. The purified H-*ras* p21 was stored at −20°C in 50 mM Tris–HCl pH 7.5, 50 mM NaCl, 1 mM $MgCl_2$, 1 μM GDP and 50% glycerol.

2.2. Native gel electrophoresis

To study the formation of the H-*ras* p21 · $CDC25^{Mm}_{1005-1260}$ complex, a native gel electrophoresis was carried out as described [23]. The stock buffer contained 90.12 g of glycine and 3 g of sodium azide adjusted to pH 8.9 with Trizma base in 6 l. The sample buffer, containing bromophenol blue, and the electrode buffer were prepared by dilution in H_2O of stock buffer (1:1 and 1:20, respectively). The gel composition was 12% acrylamide/0.27% bisacrylamide in stock buffer diluted twice and polymerized using ammonium persulfate and TEMED. A current of 20 mA per gel was applied during 1 h for the electrophoresis at 4°C. When indicated 20 μM GDP was added in the polyacrylamide gel and electrophoresis buffer. The protein p21 and the complex p21 · $CDC25^{Mm}_{1005-1260}$ were reacted with anti-H-*ras* p21 monoclonal antibodies (Santa Cruz Biotechnology). Immunoreactive bands revealed by horseradish peroxidase-conjugated anti-mouse antibodies, were developed with ECL-chemiluminescent assay system (Amersham).

2.3. GEF activity

To determine the GEF activity in vitro, the dissociation rate of the H-*ras* p21 · guanine nucleotide complexes was measured by the nitrocellulose binding assay at 30°C using [^{3}H]GDP (9.1 Ci · $mmol^{-1}$, Amersham) [24]. The H-*ras* p21 complex with [^{3}H]GDP was prepared by incubating, for 5 min at 30°C, 1 μM p21 in 50 mM Tris–HCl, pH 7.5, 0.2 mM $MgCl_2$, 100 mM NH_4Cl, 0.5 mg ml^{-1} BSA, 3 mM EDTA and 5 μM [^{3}H]GDP, followed by the addition of $MgCl_2$ (3 mM). The dissociation rate of the complex (final concentration 0.2 μM) was kinetically followed after the addition of a 1000-fold excess of unlabeled nucleotide. Aliquots (30 μl) were withdrawn at different times and the radioactive nucleotide bound to H-*ras* p21 was determined by filtration on nitrocellulose filters (Sartorius 0.45 μm). The dissociation rates of H-*ras* p21 · GDP complex was performed as indicated by Créchet et al. [26].

2.4. Circular dichroism

Circular dichroism spectra were recorded with a Jasco J700 dichrograph calibrated with a solution of ammonium D-10-camphorsulfonate according to Jasco technical specifications. All CD spectra were obtained at 24°C, using a 2 nm spectral band width and collecting points every 0.1 nm. The near-UV CD spectra (230–340 nm) were collected at a scan rate of 20 nm/min using a path length of 1.0 cm. In order to reduce the signal-to-noise ratio the spectra were obtained as the average of 10 scans. The far-UV spectra (195–250 nm) were obtained at 10 nm/min using a path length of 0.1 cm and averaging the data over two scans. The background spectra were recorded using the buffer solution (50 mM Tris–HCl pH 7.5, 50 mM NaCl, 50% glycerol) and with the same number of scans as the sample spectra.

Secondary structure estimations were computed with the Jasco SSE-338 program that compares the actual protein spectrum, from 190 to 240 nm, with reference spectra for four conformations (α-helix, β-sheet, β-turn, and random or unordered). These spectra are based on the CD spectra of 15 reference proteins with known secondary and tertiary structure [27].

2.5. Fluorescence analysis

Fluorescence measurements were performed on a Jasco FP-777 spectrofluorimeter with 1.5 nm excitation and 5 nm emission slit widths. The excitation wavelength was 280 nm and emission range monitored between 310 and 450 nm. All experiments were performed in a 1 ml fluorescence quartz cell at 27°C. Sample concentration was 0.4 μM in 50 mM Tris–HCl pH 7.5, 10 mM $MgCl_2$, 100 mM NH_4Cl [28]. The spectra were recorded on floppy disk and analyzed with 'Excel (Microsoft)' spreadsheet.

3. Results and discussion

3.1. Purification and activity of the minimal catalytic domain of CDC25^{Mm}

The active domain CDC25$^{Mm}_{1005-1260}$ was highly purified using the pMAL-cRI system (1 mg/l of cell culture). The induction temperature (28°C) and the concentration of IPTG (0.3 mM) were essential for the solubility of the protein and for its stability. All the purification steps were performed at 4°C. After chromatographic separation on amylose–resin, thrombin digestion and MonoQ-FPLC purification, CDC25$^{Mm}_{1005-1260}$ ($M_r = 30\,000$) was soluble and stable for at least 1 year in storage buffer at −20°C. The yield of the mouse protein was about 0.25–0.5 mg/l of culture and its purity was estimated to be higher than 90% as determined by SDS-PAGE and staining with Coomassie Brilliant Blue (Fig. 1).

A comparison of the specific activities of CDC25$^{Mm}_{1005-1260}$ and the fusion protein MBP-CDC25$^{Mm}_{1005-1260}$ was performed. The H-*ras* p21 · GDP dissociation rate, determined at identical molar concentration and under the same experimental conditions, showed that the minimal catalytic domain CDC25$^{Mm}_{1005-1260}$ has the same specific GEF activity as the fusion protein MBP-CDC25$^{Mm}_{1005-1260}$ (Table 1),

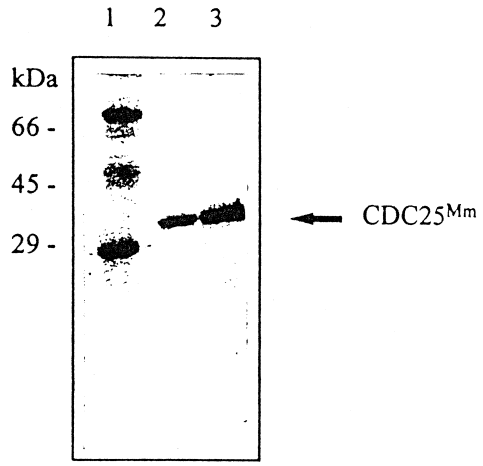

Fig. 1. SDS-PAGE analysis of purified CDC25$^{Mm}_{1005-1260}$. CDC25$^{Mm}_{1005-1260}$ was purified to homogeneity as described in Section 2. The Coomassie blue stain of the purified protein after separation by SDS polyacrylamide gel electrophoresis is shown. CDC25$^{Mm}_{1005-1260}$ (2 μg), CDC25$^{Mm}_{1005-1260}$ (4 μg) are shown in lanes 2 and 3, respectively. The molecular markers are in lane 1.

and its activity was nearly as high as that of CDC25$^{Mm}_{974-1260}$ (data not shown) [29].

3.2. Formation of the p21-CDC25^{Mm} complex on native gel electrophoresis

Purified H-*ras* p21 · GDP and CDC25$^{Mm}_{1005-1260}$ were used to evaluate their ability to form a stable complex on native gel by analyzing the mobility of H-*ras* p21. As shown on Fig. 2A when CDC25$^{Mm}_{1005-1260}$ is added (lane 2), H-*ras* p21 shows a retardation in mobility. This effect reflects the formation of the complex H-*ras* p21/CDC25$^{Mm}_{1005-1260}$ since it is not visible when CDC25$^{Mm}_{1005-1260}$ is denatured by heating prior to the loading (lane 3) or when H-*ras* p21 is loaded separately (lane 1). The heterodimer resulting from a stable interaction between H-*ras* p21 and the catalytic domain CDC25$^{Mm}_{1005-1260}$ was evidenced by Western blot analysis using monoclonal antibodies specific for H-*ras* p21. Complete inhibition of this stable complex was obtained by the addition of 20 μM GDP in the polyacrylamide gel and in the electrophoretic buffer (Fig. 2B). These results are in good agreement with those obtained with either SDC25 or CDC25^{Mm} (C-terminal domains) [24,26,31] and demonstrate that the minimal active domain in vivo is able to make a stable nucleotide-free complex with Ras. In addition, the complex can be evidenced simply by mixing equimolar amounts of H-*ras* p21 with CDC25$^{Mm}_{1005-1260}$ in a dialysis bag and removing the bound nucleotide (GDP) by electroelution (data not shown) [23].

3.3. Structural analysis of CDC25$^{Mm}_{1005-1260}$

Structural data on Ras-GEF exchange factors are not available to date. Therefore, a CD analysis on the catalytic domain CDC25$^{Mm}_{1005-1260}$ was performed to obtain structural information on this active fragment. The CD spectrum of this C-terminal domain in the far-UV regions shows the well defined features typical of proteins rich in α-helical structure, with two negative minima at 208 and 222 nm (Fig. 3A). Secondary structure calculations indicate 42% α-helix and 15% β-sheet for CDC25$^{Mm}_{1005-1260}$. These results complement and give some experimental support to predictions made by computer analysis with the

Table 1
Intrinsic and $CDC25^{Mm}_{1005-1260}$ stimulated dissociation rates of H-*ras* p21

	Dissociation rates k_{-1} (s^{-1})	Dissociation half-lives (min)
p21 · GDP	$1.4 \cdot 10^{-4}$	82.0
p21 · GDP + MBP-$CDC25^{Mm}_{1005-1260}$	$3.3 \cdot 10^{-3}$	3.45
p21 · GDP + $CDC25^{Mm}_{1005-1260}$	$5.0 \cdot 10^{-3}$	2.3

The reaction mixture contained in 500 μl of standard buffer (as described in Section 2), 1 μM H-*ras* p21 which has been preincubated for 5 min at 30°C (5 μM [^{3}H]GDP). The reaction was started by the addition of a 1000-fold excess of unlabeled nucleotide. A total of 30 μl aliquots were withdrawn, filtered and the radioactivity counted. A total of 25 nM MBP-$CDC25^{Mm}_{1005-1260}$ and 25 nM $CDC25^{Mm}_{1005-1260}$ were used. In the equation $\ln(c_t/c_o) = k_{-1} \cdot t$, c_o represents the initial concentration of the p21 nucleotide complex and c_t the concentration at time t.

method of Garnier (51% α-helix, 11% β-sheet) (program: Predict 7) [25] or the HssPred algorithm (37.5% α-helix, 27% β-sheet) (http://embl-heidelberg.de/sspred/ssp_sin.html).

The aromatic CD spectrum of $CDC25^{Mm}_{1005-1260}$ is characterized by an asymmetric band extending from about 255 nm to 300 nm, with maximum at 282 nm and poorly defined structure on its high energy tail (Fig. 3B). This band encompasses contributions from 25 aromatic amino acids (3 tryptophans, 10 tyrosines and 12 phenylalanines) in the C-terminal domain. However the shape of the CD envelope indicates that the contribution of the tyrosine residues is largely dominant [30,32]. Immobilized tryptophan residues generally give detectable contributions to the low-energy portion of the aromatic CD spectrum, since their ^1L_b transition can extend to and beyond 300 nm, often with defined vibrational structure [32–34]. Although, in principle, an accidental cancellation of the contributions from the three individual tryptophan chromophores can occur, the smooth declining of the aromatic CD curve at low energy observed here seems indicative of high conformational mobility, and hence very weak CD activity, by the tryptophan residues, suggesting they are exposed to the surface of the protein.

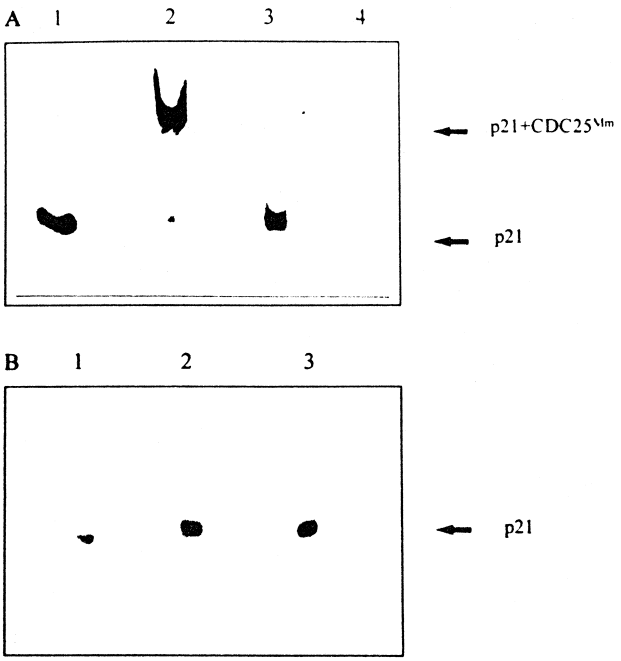

Fig. 2. Immunoblot analysis of complex formation between $CDC25^{Mm}_{1005-1260}$ and H-*ras* p21 without (A) and with 20 μM GDP (B). Lane 1: H-*ras* p21·GDP; lane 2: H-*ras* p21·GDP plus $CDC25^{Mm}_{1005-1260}$; lane 3: H-*ras* p21·GDP plus $CDC25^{Mm}_{1005-1260}$ denatured by heating; lane 4: $CDC25^{Mm}_{1005-1260}$. A total of 15 pmol of each protein were separated on native-PAGE, transferred to nitrocellulose and immunoblotted with anti-p21 monoclonal antibodies (Santa Cruz Biotechnology) and peroxidase-conjugated antibodies.

As previously discussed, $CDC25^{Mm}_{1005-1260}$ contains three tryptophan residues (w_{1054}, w_{1100}, w_{1135}), in particular the tryptophan in position 1054 is well conserved in the catalytic domain of all the known Ras-GEF proteins (Fig. 4) [19]. As illustrated on Fig. 5A upon excitation at 280 nm $CDC25^{Mm}_{1005-1260}$ shows a good fluorescence with an emission peak at 335 nm. The intensity of this peak is weakly affected by complete denaturation of the protein (Fig. 5B) suggesting that the three tryptophan residues, responsible of the fluorescence emission, could be well exposed to the solvent in the native conformation of the mouse protein [34]. This observation is in agreement with previous reported CD data in near-UV region, indicating a very low contribution of Trp residues.

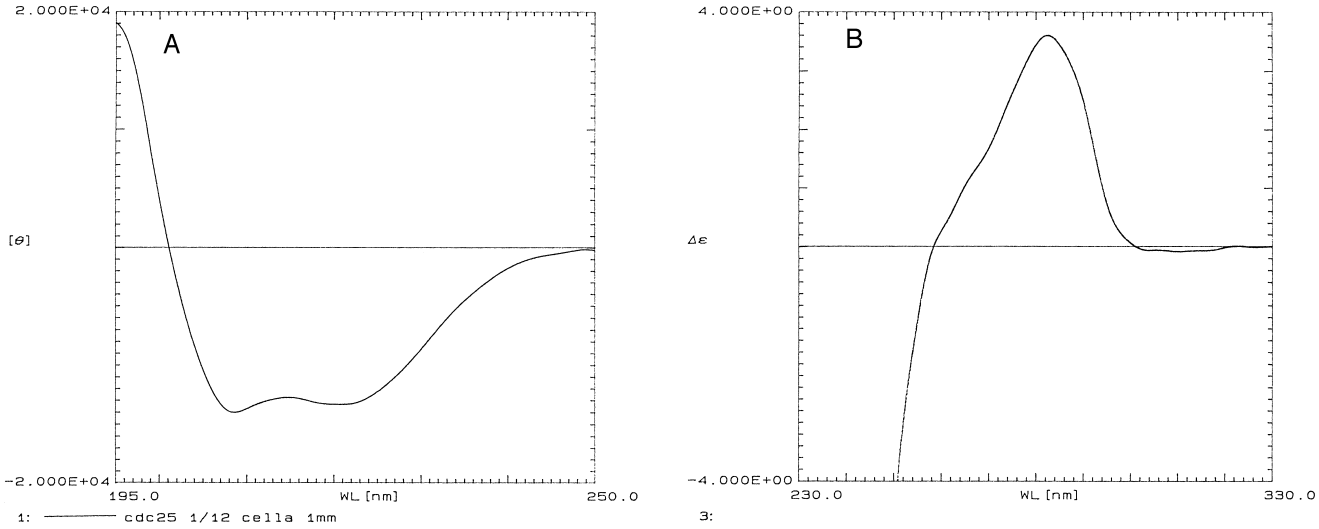

Fig. 3. (A) Plot of CD molar ellipticity in the far-UV region of $CDC25^{Mm}_{1005-1260}$. Circular dichroism analysis was as described in Section 2. A total of 3 μM $CDC25^{Mm}_{1005-1260}$ in 50 mM Tris–HCl buffer pH 7.5, 50 mM NaCl, 50% glycerol; path length 0.1 cm. The weight coefficients (percentages) for each secondary structural component of $CDC25^{Mm}_{1005-1260}$ were 42% for α-helix, 15% for β-sheet. (B) Aromatic CD spectrum of $CDC25^{Mm}_{1005-1260}$. A total of 15 μM $CDC25^{Mm}_{1005-1260}$ in the same buffer medium; path length 1.0 cm; the CD intensity was expressed in molar extinction coefficient units (M^{-1} cm^{-1}).

```
                                                                  ⬇
CDC25Mm      mleevilmtegVKTEPFENHPALEIAEQLTLLDHLVFKSIPYEEFFGQGWMKAEKYERTP   60
hgrf55       -----------VKAEPFENHSALEIAEQLTLLDHLVFKKIPYEEFFGQGWMKLEKNERTP   49
mSos1        ietfd-----------LLTLHPIEIARQLTLLESDLYRAVQPSELVGSVWTKEDKEINSP   49
Ste6         ykdel-----------VLLLPPREIAKQLCILEFQSFSHISRIQFLTKIWDnlnrfspke   49
CDC25        lkklk-----------LLDIDPYTYATQLTVLEHDLYLRITMFECLDRAWGtkycnmggs   49
                                      * **  *                 *
                                                  ⬇
CDC25Mm      YIMKTTKH-FNHVSNFIASEIIRNEDISARASAIEKWVAVADICRCLHNYNAVLEITSSI   119
hgrf55       YIMKTTKH-FNDISNLIASEIIRNEDINARVSAIEKWVAVADICRCLHNYNAVLEITSSM   108
mSos1        NLLKMIRH-TTNLTLWFEKCIVETENLEERVAVVSRIIEILQVFQELNNFNGVLEVVSAM   108
Ste6         ktstfyl--SNHLVNFVTETIVQEEEPRRRTNVLAYFIQVCDYLRELNNFASLFSIISAL   107
CDC25        pnitkfianANTLTNFVSHTIVKQADVKTRSKLTQYFVTVAQHCKELNNFSSMTAIVSAL   109
                        ⬇     *       *                 * *       *
CDC25Mm      NRSAIFRLKKTWLKVSKQTKSLLDKLQKLVSSDGRFKNLRESLRNC-DPPCVPYLGMYLT   178
hgrf55       NRSAIFRLKKTWLKVSKQTKALIDKLQKLVSSEGRFKNLREALKNC-DPPCVPYLGMYLT   167
mSos1        NSSPVYRLDHTFEQIPSRQKKILEEAHEL--SEDHYKKYLAKLRSI-NPPCVPFFGIYLT   165
Ste6         NSSPIHRLRKTWANLNSKTLASFELLNNLTEARKNFSNYRDCLENC-VLPCVPFLGVYF-   165
CDC25        YSSPIYRLKKTWDLVSTESKDLLKNLNNLMDSKRNFVKYRELLRSVtDVACVPFFGVYLS   169
               *   **                *             *       ***  * *

CDC25Mm      ---DLVFIEEGTPNYTEDGLVNFSKMRMISHIIREIRQFQQTTYKIDPQPKVIQYL--LD   233
hgrf55       ---DLAFIEEGTPNYTEDGLVNFSKMRMISHIIREIRQFQQTAYKIEHQAKVTQYL--LD   222
mSos1        NIlKTEEGNPEVLRRHGKELINFSKRRRVAEITGEIQQYQNQPYCLRVEPDIKRFF--en   223
Ste6         ---TDLTFLKTGNKDNFQNMINFDKRTKVTRILNEIKKFQSVGYMFNPINEVQELL--NE   220
CDC25        DL-TFTFVGNPDFLHNSTNIINFSKRTKIANIVEEIISFKRFHYKLKRLDDIQTVI--EA   226
                              ****      *  **       *

CDC25Mm      ESF-MLDEESLYESSLLIEPKLPT-------------------------------------   256
hgrf55       QSF-VMDEESLYESSLRIEPKLPT-------------------------------------   245
mSos1        lnpmgnsmekeftdylfnksle----------------------------------------   245
Ste6         VISRERNTNNIYQRSLTVEPRESEDQAlqrllidsgif------------------------   258
CDC25        SLENVPHIEKQYQLSLQVEPRSGNTKGsthassasgtktakflseftddkngnflklgkk   286
```

Fig. 4. Alignment of the catalytic domains of 5 *ras*-GEF proteins.Alignments were obtained with the MACAW program [35]. Residues included in the alignment for each protein are follows: mouse $CDC25^{Mm}$ ($CDC25^{Mm}$,1005–1260) human hGRF55 (hgrf55, 95–438), mouse Sos1 (mSos1, 788–1033), *Schizosaccharomyces pombe* ste6 (STE6, 654–911), *Saccharomyces cerevisiae* Cdc25 (Cdc25, 1196–1581). The tryptophan residues (w_{1054}, w_{1100}, w_{1135}) of $CDC25^{Mm}$ are pointed with an arrow and all the conservative residues of GEF-proteins are pointed with an asterisk.

Since the H-*ras* p21 protein does not have any tryptophan residues, we decided to investigate if the formation of the complex H-*ras* p21/$CDC25^{Mm}_{1005-1260}$ was accompanied by a quenching in the tryptophan fluorescence emission of the mouse protein. We observed that after the addition of purified and GDP-free H-*ras* p21 the spectrum and the intensity of $CDC25^{Mm}_{1005-1260}$ fluorescence did not significantly change, indicating that the local environment of tryptophan residues of $CDC25^{Mm}_{1005-1260}$ was not deeply affected upon interaction with H-*ras* p21. In a similar way no changes either in intensity or spectrum were observed after addition of 10 μM GDP (Fig. 6).

Taken together these data suggest that the formation of the complex H-*ras* p21/$CDC25^{Mm}_{1005-1260}$ does not modify the environment of tryptophan residues in the mouse protein, although the results of denaturation experiments strongly suggest that Trp residues are exposed to the surface of the protein and they are not involved in hydrophobic interactions.

In conclusion, this work describes for the first time the structural state of highly purified preparations of $CDC25^{Mm}_{1005-1260}$, the shortest active catalytic domain isolated so far, emphasizing the definite folded conformation of this specific GEF domain.

The availability of large amounts of purified $CDC25^{Mm}$-C domain and its ability to form a stable nucleotide-free complex with H-*ras* p21 open the way to the resolution of 3D structure of a Ras-GEF, a primary goal for the understanding of molecular mechanism of Ras activation.

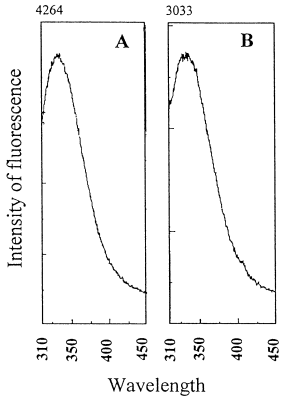

Fig. 5. Emission spectra of native $CDC25^{Mm}_{1005-1260}$ (A) and denatured $CDC25^{Mm}_{1005-1260}$ (B) 0.4 μM $CDC25^{Mm}_{1005-1260}$ in 50 mM Tris–HCl pH 7.5, 10 mM $MgCl_2$, 100 mM NH_4Cl at 27°C. The excitation wavelength is 280 nm and the emission wavelength is 335 nm. Optical bandwidths are 1.5 nm for excitation and 5 nm for emission.

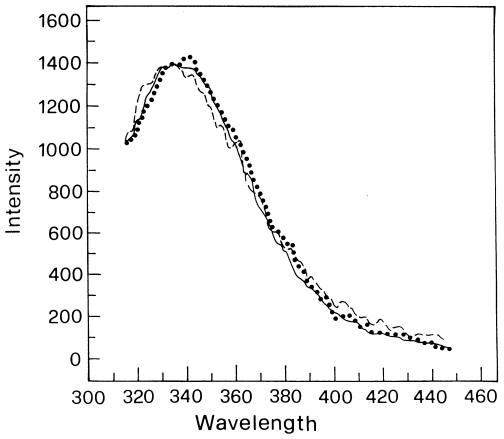

Fig. 6. Emission spectra of $CDC25^{Mm}_{1005-1260}$-H-*ras* p21 complex. $CDC25^{Mm}_{1005-1260}$ (——) $CDC25^{Mm}_{1005-1260}$ plus H-*ras* p21 (...), $CDC25^{Mm}_{1005-1260}$ plus H-*ras* p21 in presence of 10 μM GDP (---). Sample concentrations are 4 μM for $CDC25^{Mm}$ and 2 μM for H-*ras* p21. The excitation wavelength is 280 nm and the emission wavelength is 335 nm. Optical bandwidths are 1.5 nm for excitation and 5 nm for emission. From each spectrum has been subtracted the aromatic residue contribution of H-*ras* p21.

Acknowledgements

This work was partially supported by a grant CEE BIOTECH BIO2CT-930005 to L.A. and by a grant from AIRC (Italian Research Cancer Foundation). We are obliged to Drs. A. Parmeggiani and S. Baouz for fruitful discussion and advice.

References

[1] M. Barbacid, Ras genes, Annu. Rev. Biochem. 56 (1987) 779–827.
[2] H.R. Bourne, D.A. Sanders, F. McCormick, The GTPase superfamily conserved structure and molecular mechanism, Nature 349 (1991) 117–127.
[3] D. Bowtell, P. Fu, M. Simon, P. Senior, Identification of murine homologous of the *Drosophila* son of sevenless gene: potential activator of *ras*, Proc. Natl. Acad. Sci. U.S.A. 89 (14) (1992) 6511–6515.
[4] P. Chardin, J.H. Camonis, N.W. Gale, L. Van Aelst, J. Schlessinger, M.H. Wigler, D. Bar-Sagi, Human Sos1: a

guanine nucleotide factor for Ras that binds to GRB2, Science 260 (5112) (1993) 1338–1343.
[5] E. Martegani, M. Vanoni, R. Zippel, P. Coccetti, R. Brambilla, C. Ferrari, E. Sturani, L. Alberghina, Cloning by functional complementation of a mouse cDNA encoding a homologue of CDC25, a *Saccharomyces cerevisiae* Ras activator, EMBO J. 11 (6) (1992) 2151–2157.
[6] H. Cen, A.G. Papageorge, R. Zippel, D.R. Lowy, K. Zhang, Isolation of multiple mouse cDNAs with coding homology to *Saccharomyces cerevisiae* CDC25: identification of a region related to Bcr, Vav, Dbl and CDC24, EMBO J. 11 (11) (1992) 4007–4015.
[7] C. Shou, C.L. Farnsworth, B.G. Neel, L.A. Feig, Molecular cloning of a cDNA encoding a guanine nucleotide-releasing factor for Ras p21, Nature 358 (6384) (1992) 351–354.
[8] C. Ferrari, R. Zippel, E. Martegani, N. Gnesutta, V. Carrera, E. Sturani, Expression of two different products of CDC25^{Mm}, a mammalian Ras activator, during development of mouse brain, Exp. Cell. Res. 210 (2) (1994) 353–357.
[9] W. Wei, S.S. Schreiber, M. Baudry, G. Tocco, D. Broek, Localization of the cellular expression pattern of cdc25NEF and *ras* in the juvenile rat brain, Mol. Brain Res. 19 (4) (1993) 339–344.
[10] F. Schweighoffer, M. Faure, I. Fath, M.C. Chevallier-Moulton, F. Apiou, B. Dutrillaux, E. Sturani, M. Jacquet, B. Tocque, Identification of a human guanine nucleotide releasing factor (H-GRF55) specific for Ras proteins, Oncogene 8 (6) (1993) 1477–1485.
[11] W. Wei, B. Das, W. Park, D. Broek, Cloning and analysis of human cDNAs encoding a 140 kDa brain guanine nucleotide-exchange factor, cdc25GEF, which regulates the function of Ras, Gene 151 (1–2) (1994) 279–284.
[12] A. Musacchio, T. Gibson, P. Rice, J. Thompson, M. Saraste, The PH domain:a common piece in the structural patchwork of signalling proteins, Trends Biochem. Sci. 18 (9) (1993) 343–348.
[13] C.L. Farnsworth, N.W. Freshney, L.B. Rosen, A. Ghosh, M.E. Greenberg, L.A. Feig, Calcium activation of Ras mediated by neuronal exchange factor Ras-GRF, Nature 376 (6540) (1995) 524–527.
[14] K. Touhara, J. Inglese, J.A. Pitcher, G. Shou, R.D. Lefkowitz, Binding of G protein beta–gamma subunits to pleckstrin homology domain, J. Biol. Chem. 269 (4) (1994) 10217–10220.
[15] C. Shou, A. Wurmser, K.L. Suen, M. Barbacid, L.A. Feig, K. Ling, Differential response of the Ras exchange factor Ras-GRF to tyrosine kinase and G protein mediated signals, Oncogene 10 (10) (1995) 1887–1893.
[16] R. Zippel, S. Orecchia, E. Sturani, E. Martegani, The brain specific Ras exchange factor CDC25^{Mm}: modulation of its activity through Gi-protein-mediated signals, Oncogene 12 (12) (1996) 2697–2703.
[17] R.R. Mattingly, I.G. Macara, Phosphorylation-dependent activation of the Ras-GRF/CDC25^{Mm} exchange factor by muscarinic receptors and Gi-protein beta gamma subunits, Nature 382 (6588) (1996) 268–272.
[18] M.S. Boguski, F. McCormick, Proteins regulating Ras and its relatives, Nature 366 (6456) (1993) 643–654.
[19] E. Martegani, M. Vanoni, R. Zippel, E. Sturani. L. Alberghina, in: M. Zerial, L.A. Huber (Eds.), Guidebook to the Small GTPases, 1995, pp. 126–130.
[20] R. Zippel, C. De Maddalena, G. Porro, D. Modena, M. Vanoni, Increased p21*ras*-specific guanine nucleotide exchange causes tumor formation in nude mice, Int. J. Oncol. 4 (1994) 175–179.
[21] P. Coccetti, I. Mauri, L. Alberghina, E. Martegani, A. Parmeggiani, The minimal active domain of the mouse Ras exchange factor CDC25^{Mm}, Biochem. Biophys. Res. Commun. 206 (1995) 253–259.
[22] M.Y. Mistou, E. Jacquet, P. Poullet, H. Rensland, P. Gideon, I. Schlichting, A. Wittinghofer, A. Parmeggiani, Mutations of Ha-ras p21 that define important regions for the molecular mechanism of the SDC25 C-domain, a guanine nucleotide dissociation stimulator. EMBO J. 11 (1992) 2391–2398.
[23] E. Jacquet, S. Baouz, A. Parmeggiani, Characterization of mammalian C-CDC25^{Mm} exchange factor and kinetic properties of the exchange reaction intermediate p21 · C-CDC25^{Mm}, Biochemistry 34 (38) (1995) 12347–12354.
[24] E. Jacquet, M.C. Parrini, A. Bernardi, E. Martegani, A. Parmeggiani, Properties of the catalytic domain of CDC25, a *Saccharomyces cerevisiae* GDT/GTP exchange factor: comparison of its activity on full length and C-terminal truncated Ras2 proteins, Biochem. Biophys. Res. Commun. 199 (2) (1994) 497–503.
[25] R.S. Carmenes, J.P. Freije, M.M. Molina, J.M. Martin, Predict 7, a program for protein structure prediction, Biochem. Biophys. Res. Commun. 159 (1989) 687–693.
[26] J.B. Créchet, P. Poullet, J. Camonis, M. Jacquet, A. Parmeggiani, A different kinetic properties of the two mutants, RAS2Ile152 and RAS2Val19, that suppress the CDC25 requirement in RAS/adenylate cyclase pathway in *Saccharomyces cerevisiae*, J. Biol. Chem. 265 (1990) 1563–1568.
[27] J.T. Yang, C.S. Wu, H.M. Martinez, Calculation of protein conformation from circular dichroism, Meth. Enzymol. 130 (1986) 208–269.
[28] B. Antonny, P. Chardin, M. Roux, M. Chabre, GTP hydrolysis mechanism in *ras* p21 and in the *ras*-GAP complex studied by fluorescence measurements on tryptophan mutants, Biochemistry 30 (1991) 8287–8295.
[29] E. Jacquet, M. Vanoni, C. Ferrari, L. Alberghina, E. Martegani, A. Parmeggiani, A mouse CDC25-like product enhances the formation of the active GTP complex of human *ras* p21 and *Saccharomyces cerevisiae* Ras2 proteins, J. Biol. Chem. 267 (34) (1992) 24181–24183.
[30] P.C. Kahn, The interpretation of the near-ultraviolet circular dichroism, Meth. Enzymol. 61 (1979) 339–378.
[31] P. Poullet, J. Crèchet, A. Bernardi, A. Parmeggiani, Properties of the catalytic domain of Sdc25p, a yeast GDP/GTP exchange factor of Ras properties. Complexation with wild type Ras2p,[S24N]Ras2p and [R80D,N81D]Ras2p, Eur. J. Biochem. 227 (1995) 537–544.

[32] E.H. Strickland, Aromatic contributions to circular dichroism spectra of proteins, CRC Crit. Rev. Biochem. 2 (1974) 113–175.
[33] M. Beltramini, L. Bubacco, B. Salvato, L. Casella, M. Gullotti, S. Garofani, The aromatic circular dichroism spectrum as a probe for conformational changes in the active site environment of hemocyanins, Biochim. Biophys. Acta 1120 (1992) 24–32.
[34] J.G. McAfee, S.P. Eemondson, P.K. Datta, J.W. Shriver, R. Gupa, Gene cloning, expression and characterization of the Sac7 proteins from the hyperthermophile *Sulfolobus acidocaldarius*, Biochemistry 34 (1995) 10063–10077.
[35] G.D. Schuler, S.F. Altschul, D.J. Lipman, A workbench for multiple alignment construction and analysis, Prot. Funct. Genet. 9 (1991) 180–190.